SPIE Proceedings Vol 2657, paper # 44, Human Vision and Electronic Imaging, B. Rogowitz and J. Allebach, Ed., The Society for Imaging Science and Technology, (1996).

# VISUAL THRESHOLDS FOR WAVELET QUANTIZATION ERROR

Andrew B. Watson<sup>•</sup>,<sup>a</sup>, Gloria Y. Yang<sup>•</sup>,<sup>b</sup>, Joshua A. Solomon<sup>•</sup>,<sup>c</sup> & John Villasenor<sup>•</sup>,<sup>d</sup>

NASA Ames Research Center, Moffett Field, CA, 94035-1000
 Department of Electrical Engineering, UCLA, Los Angeles, CA 90024-1594

## ABSTRACT

The Discrete Wavelet Transform (DWT) decomposes an image into bands that vary in spatial frequency and orientation. It is widely used for image compression. Measures of the visibility of DWT quantization errors are required to achieve optimal compression. Uniform quantization of a single band of coefficients results in an artifact that is the sum of a lattice of random amplitude basis functions of the corresponding DWT synthesis filter, which we call *DWT uniform quantization noise*. We measured visual detection thresholds for samples of DWT uniform quantization noise in Y, Cb, and Cr color channels.

The spatial frequency of a wavelet is  $r 2^{-L}$ , where r is display visual resolution in pixels/degree, and L is the wavelet level. Amplitude thresholds increase rapidly with spatial frequency. Thresholds also increase from Y to Cr to Cb, and with orientation from low-pass to horizontal/vertical to diagonal.

We propose a mathematical model for DWT noise detection thresholds that is a function of level, orientation, and display visual resolution. This allows calculation of a "perceptually lossless" quantization matrix for which all errors are in theory below the visual threshold. The model may also be used as the basis for adaptive quantization schemes.

## **KEY WORDS**

wavelet, human, visual perception, quantization, compression, image, subband coding, vision, perceptually lossless, perfect reconstruction filter bank

## **1. INTRODUCTION**

NASA's extensive image compression requirements may be met in part by the use of wavelet techniques.<sup>1</sup> Wavelets form a large class of signal and image transforms, generally characterized by decomposition into a set of self-similar signals that vary in scale and (in 2D) orientation.<sup>2</sup> The Discrete Wavelet Transform (DWT) is a particular member of this family which operates on discrete sequences, and which has proven to be an effective tool in image

<sup>&</sup>lt;sup>a</sup> beau@vision.arc.nasa.gov, http://vision.arc.nasa.gov/

<sup>&</sup>lt;sup>b</sup> Current address: 1510 Page Mill Road, MS 10, Palo Alto, CA 94304, gloriay@vnet.ibm.com

<sup>&</sup>lt;sup>c</sup> Current address: Institute of Ophthalmology, Bath Street, London EC1V 9EL, j.solomon@ucl.ac.uk

<sup>&</sup>lt;sup>d</sup> villa@icsl.ucla.edu

Watson

compression.<sup>3, 4, 5, 6</sup> In a typical compression application, an image is subjected to a twodimensional DWT whose coefficients are then quantized and entropy coded.

DWT compression is lossy, and depends for its success upon the invisibility of the artifacts. The purpose of this paper is to provide information on the visibility of DWT artifacts, and to show how it may be used in the design of wavelet compression systems. In this research we have generally followed earlier work on the Discrete Cosine Transform<sup>7, 8, 9</sup>, with some important differences that will be discussed below.

## 2. BACKGROUND

# 2.1. Discrete Wavelet Transform

Figure 1 illustrates the elements of a one-dimensional, two-channel perfectreconstruction filter bank. The input discrete sequence  $\mathbf{x}$  is convolved with high-pass and low-pass analysis filters  $\mathbf{a}_H$  and  $\mathbf{a}_L$ , and each result is down-sampled by two, yielding the transformed signals  $\mathbf{x}_H$  and  $\mathbf{x}_L$ . The signal is reconstructed through up-sampling and convolution with high and low synthesis filters  $\mathbf{s}_H$  and  $\mathbf{s}_L$ . For properly designed filters, the signal  $\mathbf{x}$  is reconstructed exactly  $(\mathbf{y}=\mathbf{x})$ .

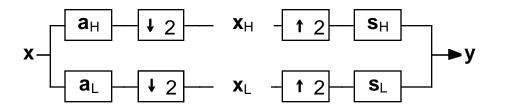


Figure 1. A two-channel perfect-reconstruction filter bank.

A DWT is obtained by further decomposing the low-pass signal  $x_L$  by means of a second identical pair of analysis filters, and, upon reconstruction, synthesis filters, as shown in Figure 2. This process may be repeated, and the number of such stages defines the *level* of the transform.

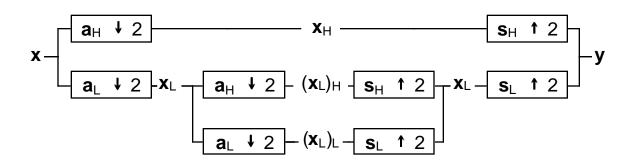


Figure 2. Two-level 1D Discrete Wavelet Transform.

With two-dimensional signals such as images, the DWT is typically applied in a separable fashion to each dimension. Now each filter is two-dimensional, with the subscript indicating the separable horizontal and vertical components, and the downsampling operation is applied in both dimensions. As in the one-dimensional case, the process may be repeated a number of times, in each case by applying the component  $\mathbf{x}_{LL}$  as input to a second stage of identical filters.

Here we adopt the term *level* to describe the number of 2D filter stages a component has passed through, and the term *orientation* to identify the four possible combinations of low-pass and high-pass filtering the signal has experienced. We index orientations as follows:  $\{1,2,3,4\} = \{LL,HL,HH,LH\}$  where low and high are in the order horizontal-vertical. Each combination of level and orientation  $\{L,O\}$  specifies a single *band*. For the purpose of this research we selected the 9-7 tap Antonini biorthogonal filters.<sup>4</sup>

# 2.2. DWT Quantization Matrix

Compression of the DWT is achieved by quantization and entropy coding of the DWT coefficients. Typically a uniform quantizer is used, implemented by division by a factor Q and rounding to the nearest integer. The factor Q may differ for different bands. It will be convenient to speak of a *quantization matrix* to refer to a set of quantization factors corresponding to a particular matrix of levels and orientations.

A particular quantization factor Q in one band will result in coefficient errors in that band that are approximately uniformly distributed over the interval [-Q/2, Q/2]. The error image will be the sum of a lattice of basis functions with amplitudes proportional to the corresponding coefficient errors. To predict the visibility of the error due to a particular Q, we must measure the visibility thresholds for individual basis functions and error ensembles.

## 2.3. Display Visual Resolution

Visibility of DWT basis functions will depend upon display visual resolution in pixels/degree. Given a viewing distance v in cm and a display resolution d in pixels/cm, the effective display visual resolution (DVR) r in pixels/degree of visual angle is

$$r = d v \tan(\pi/180) \approx d v \pi/180$$
 (1)

# 2.4. Wavelet Level and Spatial Frequency

A single basis function encompasses a band of spatial frequencies. We take the Nyquist frequency of the display resolution as the nominal spatial frequency of the first DWT level, and the frequency of each subsequent level will be reduced by a factor of two. Thus for a display resolution of r pixels/degree, the spatial frequency f of level L will be

$$f = r 2^{-L}$$
 cycles/degree (2)

## **3. METHODS**

Stimuli were modulations of either Y, Cb, or Cr channels of a color image. These produce images that are black/white, yellow/purple, and red/green respectively. All modulations were added to an otherwise uniform (YCbCr =  $\{128,0,0\}$ ) image of size 1024x1024 pixels.

Modulations were either single DWT basis functions or samples of DWT uniform quantization noise, as shown in Figure 3. We created images of basis functions by setting to one a single coefficient in band  $\{L,0\}$  in an otherwise zero DWT (Figure 3a), and computing the inverse DWT. Images of DWT noise were produced by filling one band of an otherwise zero DWT with samples drawn uniformly from the interval [-1,1] (Figure 3c) and inverse transforming the result.

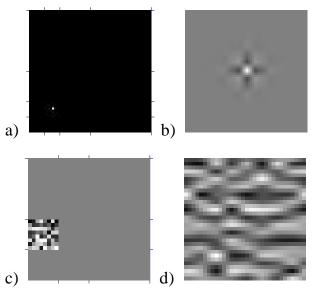


Figure 3. Example stimuli: a) basis function DWT, b) basis function, image size 64x64, c) noise DWT, d) noise, image size 32x32.

Individual modulation images were scaled to produce amplitudes in the range of [0,126]. The amplitude of the modulated signal is our measure of stimulus intensity. The modulated channel, plus the two remaining unmodulated channels, were then transformed to R'G'B' using the rule

$$\begin{bmatrix} R' \\ G' \\ B' \end{bmatrix} = \begin{bmatrix} 1 & 0 & 1.402 \\ 1 & -0.3441 & -0.7141 \\ 1 & 1.772 & 0 \end{bmatrix} \begin{bmatrix} Y \\ C_b - 128 \\ C_r - 128 \end{bmatrix}$$
(3)

To vary the display visual resolution we pixel-replicated the stimuli by factors of 1 (no replication), 2, or 4 in both dimensions, yielding visual resolutions of 64, 32, and 16 pixels/degree. For all stimuli, the duration was 16 frames in duration at a frame rate of 60 Hz, or 267 msec. The time course was a Gaussian  $e^{-\pi (f/8)^2}$  where f is in frames. To measure detection thresholds for individual stimuli we used an adaptive two-alternative forced-choice (2AFC) procedure.<sup>10</sup> Three observers took part in the experiments. Observer gyy was a 23 year old female corrected myope, sfl was a 21 year old male emmetrope, and observer abw was a 43 year old corrected myope.

#### 4. **RESULTS**

## 4.1. Effect of DWT Level

Thresholds for display resolutions of 16, 32, and 64 pixels/degree, all at orientation 4, are shown in Figure 4. In general thresholds are largely unaffected by resolution, once they are

expressed as a function of spatial frequency in cycles/degree. Additional data from observer sfl confirm this observation.

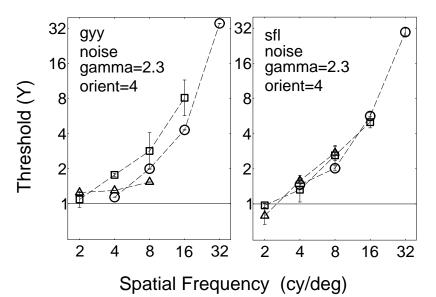
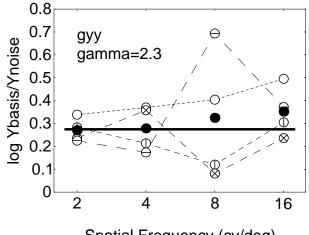


Figure 4. Thresholds at display resolutions of 16 (triangles) 32 (squares) and 64 pixels/degree (circles), for orientation 4.

# 4.2. Single Basis Functions vs Noise Images

Figure 5 plots the difference between log thresholds for single basis functions and for noise. As expected, basis function thresholds are uniformly higher than noise thresholds. We considered a simple spatial probability summation model to account quantitatively for the difference between basis function and noise thresholds.<sup>11, 12</sup> In this context, this model asserts that the Minkowski sum over individual basis functions amplitudes is equal for all basis functions ensembles at threshold. This prediction is plotted as the horizontal line in Figure 5. It is clear that probability summation provides an excellent account of the difference between basis and noise thresholds.



Spatial Frequency (cy/deg)

Figure 5. Difference between log thresholds for DWT noise and basis functions. Open symbols show data for individual orientations, solid symbols are means. Heavy line is the probability summation prediction.

# 4.3. Grayscale Model

One model that provides a reasonable fit to thresholds for grayscale DWT is

$$\log Y = \log a + k \left(\log f - \log g_O f_0\right)^2 \quad . \tag{4}$$

This is a parabola in log Y vs log f coordinates, with a minimum at  $g_O f_O$  and a width of  $k^2$ . The term  $g_O$  shifts the minimum by an amount that is a function of orientation, and where  $g_2 = g_4 = 1$ . The term a defines the minimum threshold. The optimized parameters and rms error (of log Y) are given in Table 3. The fit is shown in Figure 6.

Color	Observer	r m s	а	k	$f_0$	<i>81</i>	83
Y	gyy & sfl	0.134	0.495	0.466	0.401	1.501	0.534

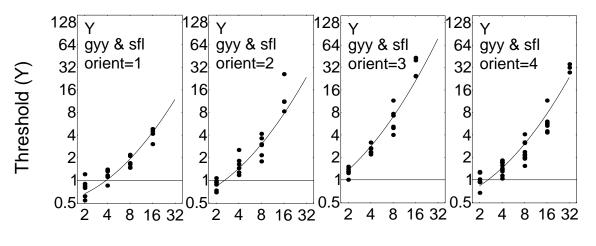


Table	3.	Parameters	for	DWT	threshold	model	for	the	Y	channel.
-------	----	------------	-----	-----	-----------	-------	-----	-----	---	----------

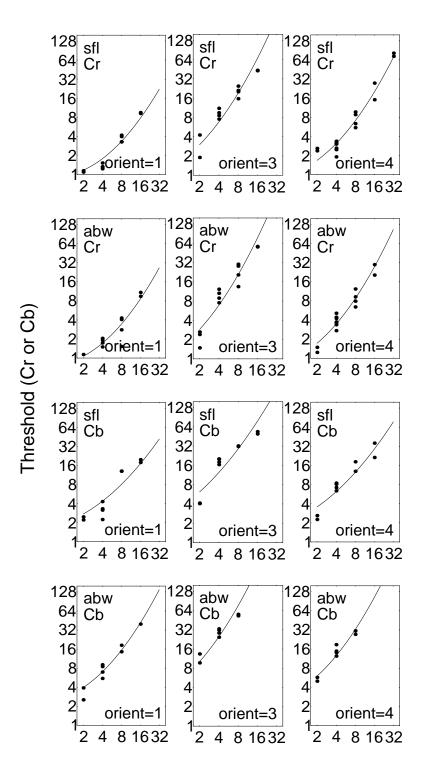
# Spatial Frequency (cy/deg)



## 4.4. Color Results and Model

Figure 7 shows results for observers sfl and abw at orientations 1, 3, and 4 for a DWT noise pattern and display gamma of 2.3.

We have applied the same model used for grayscale thresholds to the color thresholds in Figure 7. The solid curves therein show the various fits. The parameters are in Table 4, along with the Y parameters from Table 3.



Spatial Frequency (cy/deg)

Figure 7. Thresholds for DWT uniform noise in Cr and Cb channels..

Color	Observer	r m s	а	k	$f_0$	81	83
Y	gyy & sfl	0.134	0.495	0.466	0.401	1.501	0.534
Cr	sfl	0.113	0.944	0.521	0.404	1.868	0.516
	abw	0.127	0.803	0.539	0.328	2.017	0.589
Cb	sfl	0.145	1.633	0.353	0.209	1.520	0.502
	abw	0.093	2.432	0.520	0.269	1.706	0.599

Table 4. Parameters for DWT YCbCr threshold model.

# 5. QUANTIZATION MATRICES

We now use the model developed above to compute a "perceptually lossless" quantization matrix, by using a quantization factor for each level and orientation that will result in a quantization error that is just at the threshold of visibility. For uniform quantization and a given quantization factor Q, the largest possible coefficient error is Q/2. The amplitude of the resulting noise is approximately  $A_{L,O}$  Q/2. Thus we set

$$Q_{L,O} = 2 Y_{L,O} / A_{L,O}$$
(5)

The basis function amplitudes  $A_{L,O}$  are given for six levels in Table 5.

	Level							
Orientation	1	2	3	4	5	6		
1	0.62171	0.345374	0.18004	0.0914012	0.0459435	0.0230128		
2	0.672341	0.413174	0.227267	0.117925	0.0597584	0.0300184		
3	0.727095	0.494284	0.286881	0.152145	0.0777274	0.0391565		
4	0.672341	0.413174	0.227267	0.117925	0.0597584	0.0300184		

Table 5. Basis function amplitudes  $A_{L,O}$  for a six-level Antonini DWT.

Combining (4), (5), and (2),

$$Q_{L,O} = \frac{2}{A_{L,O}} a \, 10^{k \left( \log \frac{2^L f_0 g_O}{r} \right)^2} \tag{6}$$

Table 6 shows example matrices computed from this formula.

		Level					
Color	Orientation	1	2	3	4		
Y	1	14.049	11.106	11.363	14.5		
	2	23.028	14.685	12.707	14.156		
	3	58.756	28.408	19.54	17.864		
	4	23.028	14.685	12.707	14.156		
Cb	1	55.249	46.559	48.45	59.988		
	2	86.789	60.485	54.571	60.476		
	3	215.84	117.45	86.737	81.231		
	4	86.789	60.485	54.571	60.476		
Cr	1	25.044	19.282	19.665	25.597		
	2	60.019	34.335	27.276	28.55		
	3	184.64	77.569	47.441	39.468		
	4	60.019	34.335	27.276	28.55		

Table 6. Quantization factors for four-level Antonini DWT for r=32 pixel/degree.

Figure 8 shows an example image compressed using the quantization matrix of Table 6, and twice that matrix. Viewed from the appropriate distance (24 inches, approximately arm's length) the quantization artifacts should be invisible for the left image, and visible for the right. Using typical entropy coding techniques, the resulting bitrates for these two examples are 1.05 and 0.67 bits/pixel.



Figure 8. Image compressed with perceptually lossless DWT quantization matrix (left) and twice that matrix (right). Image dimensions are 256x256 pixels. Quantization matrix is designed for a viewing distance of 24 inches.

The quantization matrix is inevitably a function of the display visual resolution, as is evident from (6). Figure 9 shows Y quantization factors for display visual resolutions of 16,

32, and 64 pixels/degree. These figures show that for low visual resolution (16 pixels/degree), the quantization factors are small and almost invariant with level and orientation. At the middle resolution, typical of office viewing of desktop computer images, the function is still a rather flat function of level for all orientations except 3, which shows a large elevation at the lowest level. At the highest visual resolution, oblique horizontal, and vertical factors are strong functions of level, while the reference signal is still nearly invariant with level.

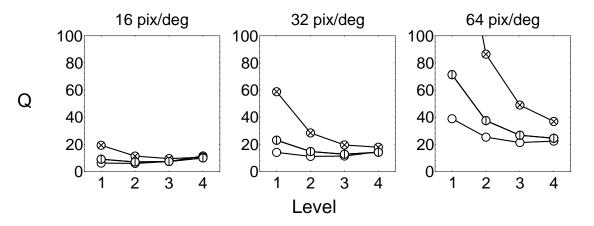


Figure 9. Quantization matrices for three display visual resolutions plotted as functions of level and orientation.

## 6. CONCLUSIONS

We have measured visual thresholds for samples of uniform quantization noise of a DWT based on the Antonini wavelet. Thresholds were collected for gamma-corrected signals in the three channels of the YCbCr color space. We propose a mathematical model for the thresholds, which may be used to design a simple "perceptually lossless" quantization matrix, or which may be used to weight quantization errors or masking backgrounds in more elaborate adaptive quantization schemes. These perceptual data, models, and methods may enhance the performance of wavelet compression schemes.

## 7. ACKNOWLEDGMENTS

This work was supported by NASA Grant 199-06-12-39 to Andrew Watson from the Life and Biomedical Sciences and Applications Division. We thank Albert J. Ahumada and Heidi A. Peterson for useful discussions, and Stephan Legeny for diligent observations.

### 8. **REFERENCES**

- 1. A. Jaworski, "Earth Observing System (EOS) Data and Information System (DIS) software interface standards," AIAA/NASA Second International Symposium on Space Information Systems, Proceedings, AIAA-90-5075, (1990).
- 2. S.G. Mallat, "Multifrequency channel decompositions of images and wavelet models," IEEE Transactions on Acoustics, Speech, and Signal Processing, 37(12), 2091-2110 (1989).

- 3. T. Hopper, C. Brislawn and J. Bradley, "WSQ grey-scale fingerprint image compression specification, Version 2.0," Criminal Justice Information Services, Federal Bureau of Investigation, Washington, DC. (1993).
- 4. M. Antonini, M. Barlaud, P. Mathieu and I. Daubechies,"Image coding using the wavelet transform," IEEE Transactions on Image Processing, 1, 205-220 (1992).
- 5. J.M. Shapiro,"An embedded wavelet hierarchical image coder," ICASSP, 657-660 (1992).
- 6. J. Villasenor, B. Belzer and J. Liao,"Wavelet filter evaluation for efficient image compression," IEEE Transactions on Image Processing, 4, 1053-1060 (1995).
- 7. H. Peterson, A.J. Ahumada, Jr. and A. Watson,"An Improved Detection Model for DCT Coefficient Quantization," SPIE Proceedings, 1913, 191-201 (1993).
- A.B. Watson, "DCT quantization matrices visually optimized for individual images," Human Vision, Visual Processing, and Digital Display IV, Proceedings of the SPIE, 1913, 202-216 (1993).
- 9. A.B. Watson, J.A. Solomon and A.J. Ahumada, Jr., "The visibility of DCT basis functions: effects of display resolution," Proceedings Data Compression Conference, J. A. Storer and M. Cohn, , 371-379, IEEE Computer Society Press, Los Alamitos, CA (1994).
- 10. A.B. Watson and D.G. Pelli,"QUEST: A Bayesian adaptive psychometric method," Perception and Psychophysics, 33(2), 113-120 (1983).
- 11. J.G. Robson and N. Graham,"Probability summation and regional variation in contrast sensitivity across the visual field," Vision Research, 21, 409-418 (1981).
- 12. A.B. Watson,"Probability summation over time," Vision Research, 19, 515-522 (1979).